This article was downloaded by:
On: *26 January 2011*
Access details: *Access Details: Free Access*
Publisher *Taylor & Francis*
Informa Ltd Registered in England and Wales Registered Number: 1072954 Registered office: Mortimer House, 37-41 Mortimer Street, London W1T 3JH, UK

Liquid Crystals
Publication details, including instructions for authors and subscription information:
http://www.informaworld.com/smpp/title~content=t713926090

Optical properties of frustrated cholesteric liquid crystals

P. Ribière[a]; S. Pirkl[ab]; P. Oswald[a]
[a] École Normale Supérieure de Lyon, Laboratoire de Physique 46, Lyon Cedex 07, France [b] University of Chemical Technology, Pardubice, Czech Republic

To cite this Article Ribière, P. , Pirkl, S. and Oswald, P.(1994) 'Optical properties of frustrated cholesteric liquid crystals', Liquid Crystals, 16: 2, 203 — 221
To link to this Article: DOI: 10.1080/02678299408029147
URL: http://dx.doi.org/10.1080/02678299408029147

PLEASE SCROLL DOWN FOR ARTICLE

Full terms and conditions of use: http://www.informaworld.com/terms-and-conditions-of-access.pdf

This article may be used for research, teaching and private study purposes. Any substantial or systematic reproduction, re-distribution, re-selling, loan or sub-licensing, systematic supply or distribution in any form to anyone is expressly forbidden.

The publisher does not give any warranty express or implied or make any representation that the contents will be complete or accurate or up to date. The accuracy of any instructions, formulae and drug doses should be independently verified with primary sources. The publisher shall not be liable for any loss, actions, claims, proceedings, demand or costs or damages whatsoever or howsoever caused arising directly or indirectly in connection with or arising out of the use of this material.

LIQUID CRYSTALS, 1994, VOL. 16, NO. 2, 203–221

Optical properties of frustrated cholesteric liquid crystals

by P. RIBIÈRE, S. PIRKL† and P. OSWALD*

École Normale Supérieure de Lyon, Laboratoire de Physique 46, Allée d'Italie, 69364 Lyon Cedex 07, France

(*Received 5 April 1993; accepted 24 June 1993*)

In a previous article, we proposed a model to explain the unwinding transition in an electric field of a frustrated cholesteric liquid crystal sandwiched between two glass plates imposing a homeotropic anchoring. We found that three distinct solutions exist in materials of negative dielectric anisotropy: first, the homeotropic nematic at small thickness and small voltage, second, a translationally invariant configuration (TIC) at large voltage and, third, the cholesteric fingers. In this article, we study some optical properties of these solutions. We show first that the TIC rotates the polarization of light. Its 'apparent' rotatory power is calculated exactly and is compared with the experimental data when the TIC–nematic phase transition is second order. The agreement between theory and experiment is excellent. We show in particular that there exist discrete values of the voltage for which the TIC has a pure rotatory power. We then calculated the optical contrast of the fingers when they are observed between crossed polarizers. The agreement with experiment is still satisfactory, in spite of the approximate form of the director field chosen to describe the topology of the finger.

Downloaded At: 10:52 26 January 2011

1. Introduction

Optical properties of free cholesteric liquid crystals have been studied since the beginning of this century [1–5]. These studies do not apply to cholesteric liquid crystals in an electric field or confined between two closely spaced glass plates which strongly anchor the molecules, because these constraints alter the molecular organization. With homeotropic anchoring (i.e. when the molecules are perpendicular to the glass plates), the topological incompatibility between the simple helicoidal structure of the cholesteric and the boundary conditions leads to various molecular configurations. Let d be the sample thickness and p the quiescent cholesteric pitch. In a material of negative dielectric anisotropy ε_a, the molecules prefer to align perpendicularly to the electric field, i.e. parallel to the electrodes. Three stable configurations of the director are commonly observed, depending on the frustration ratio $C=d/p$ and on the A.C. applied voltage V between the two electrodes limiting the sample [6]. If the sample is thin enough and the electric field not too large, the cholesteric unwinds completely, leading to a *homeotropic nematic* phase. In contrast, a *translationally invariant configuration* (TIC in the following) is always the final outcome when the voltage is sufficiently large. For intermediate voltages and thick enough samples, a periodic phase consisting of parallel *cholesteric fingers* develops (see figure 1). From these observations, it was possible to construct an experimental phase diagram in the (C, V)

* Author for correspondence.

† Permanent address: University of Chemical Technology, 532 10 Pardubice, Czech Republic.

0267–8292/94 $10·00 © 1994 Taylor & Francis Ltd.

parameter plane (see figure 2). The material chosen was a mixture of the chiral material S811 (0·792 per cent wt.) and the nematic ZLI 2806 (both from E. Merck). In order to explain these observations, we used a two-order-parameter model [6] which allowed us to re-compute the main characteristics of the experimental phase diagram. This model is nevertheless approximate and is based on a topological construction of the solutions on the unit sphere, a method that was first proposed for cholesterics by Lequeux [7]. To test the relevance of this geometrical approach, we have calculated some optical properties of the molecular configurations used theoretically to determine the phase diagrams. Then, we have compared these predictions with experiment.

The organization of the article is as follows. In § 2, we briefly recall the Poincaré representation of light polarization on the unit sphere [8]. In § 3, we calculate how the polarization of the light rotates when it crosses the TIC. We shall show that the TIC possesses a *true* rotatory power only for particular values of the electric field and the

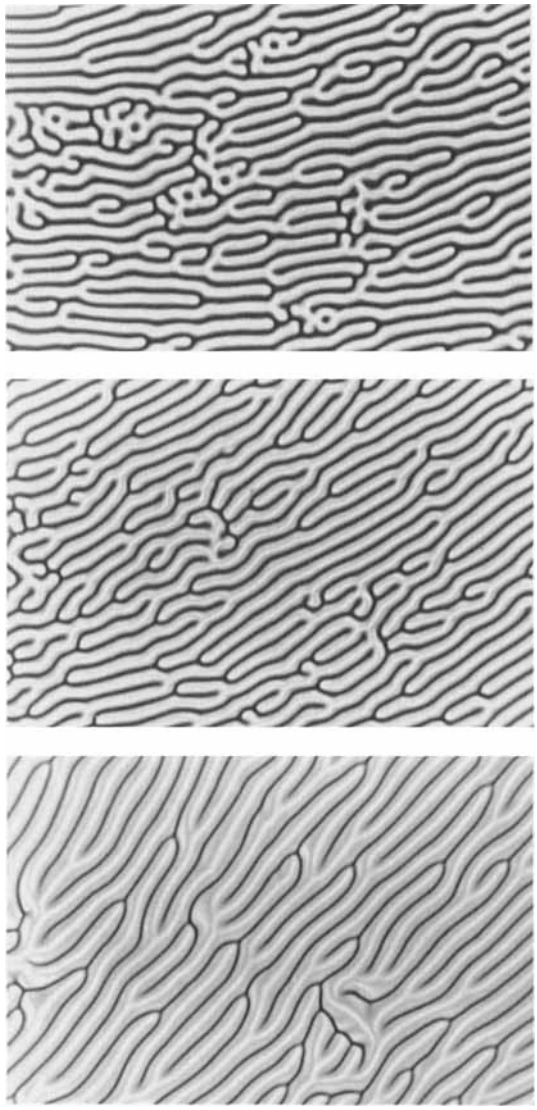

(*a*)

(*b*)

(*c*)

Downloaded At: 10:52 26 January 2011

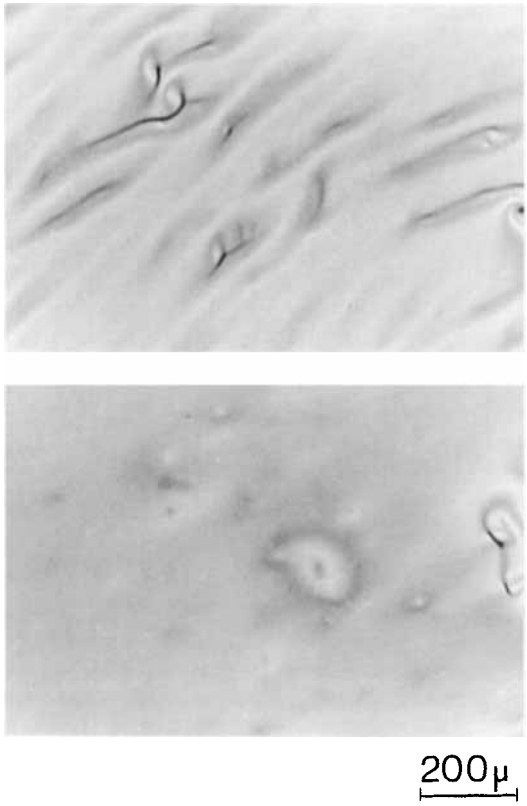

Figure 1. Two different textures (fingers and TIC) observed between crossed polarizers for the mixture ZLI 2806 + S811. $C = 0{\cdot}895$. (*a*) 1·1 V, (*b*) 1·4 V, (*c*) 2·0 V, (*d*) 2·2 V and (*e*) 2·7 V.

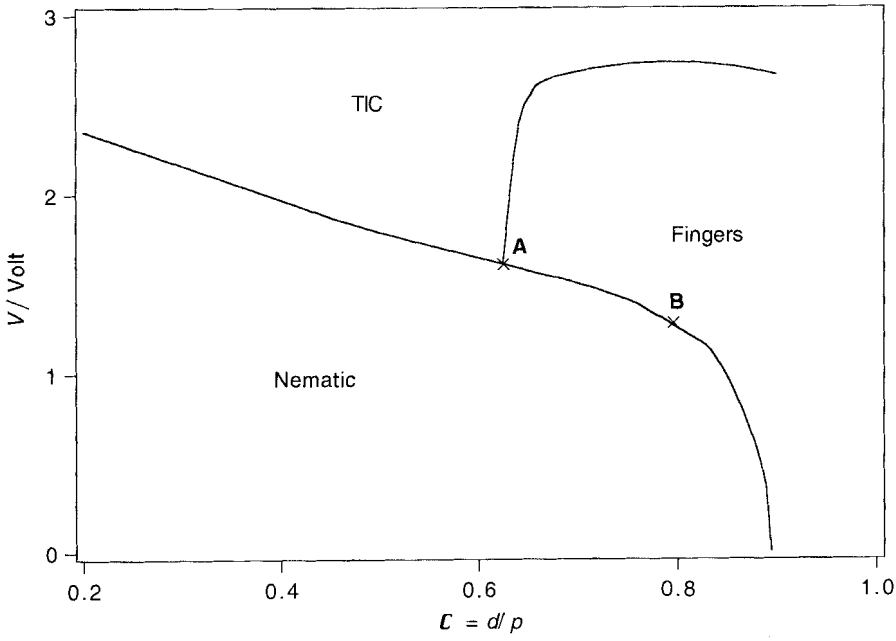

Figure 2. Simplified experimental phase diagram for ZLI 2806 + S811 (from [6]). Point *A* is a triple point where the TIC, the nematic and the fingers coexist. Between *A* and *B* the nematic–finger transition is second order, whereas it is first order to the right of *B*: point *B* is thus a Landau tricritical point.

Downloaded At: 10:52 26 January 2011

sample thickness. In § 4, we calculate the optical contrast of the fingers when they are observed between crossed polarizers. All of these results will be compared with our observations through the microscope. For simplicity, we shall only consider the case where light propagates perpendicularly to the glass plates bounding the sample (normal illumination).

2. Representation of the light polarization on the Poincaré sphere

We consider a monochromatic planar elliptically polarized wave propagating along the z axis in a one-dimensional birefringent medium i.e. translationally invariant in the x,y-plane perpendicular to z. Since

$$\operatorname{div} \mathbf{D} = 0, \tag{1}$$

one gets $D_z = 0$. In general, the E_z component does not vanish, except if the medium is isotropic. Nevertheless, it is possible to calculate E_z from E_x and E_y, using equation (1) and the constitutive relation

$$\mathbf{D} = \varepsilon \mathbf{E} \tag{2}$$

The end of the **E** component perpendicular to z traces an elliptical path as a function of time

$$\begin{cases} E_x = \cos\lambda \cos\theta \cos\omega t - \sin\lambda \sin\theta \sin\omega t, \\ E_y = \cos\lambda \sin\theta \cos\omega t + \sin\lambda \cos\theta \sin\omega t. \end{cases} \tag{3}$$

In (3), θ is the polarization angle between the x axis and the μ axis (see figure 3), while the angle λ characterizes the ellipticity of the polarization. The multiplicative constant is omitted. If $\lambda = n\pi$ or $\lambda = \pi/2 + n\pi$, $n \in Z$, the light is linearly polarized, whereas it is circularly polarized when $\lambda = \pi/4 + n\pi/2$.

On the unit sphere S^2 (usually called the Poincaré sphere), let us consider the point M defined by its longitude 2θ and its latitude 2λ (see figure 4). Set $\mathbf{u} = \mathbf{OM}$. There is a one-to-one correspondence between the Poincaré sphere and the set of all possible vibrations. It is therefore convenient to describe the different vibrations by points on S^2. Note that the poles of the sphere correspond to (left or right) circularly polarized vibrations, while the equator corresponds to linear vibrations.

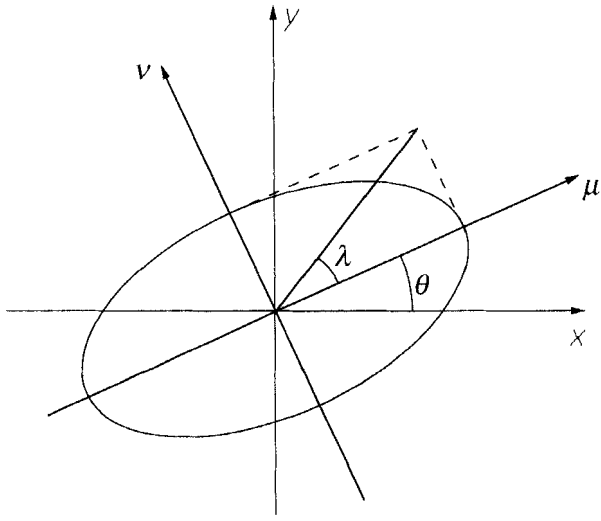

Figure 3. The two angles λ and θ characterizing an elliptically polarized planar wave.

Downloaded At: 10:52 26 January 2011

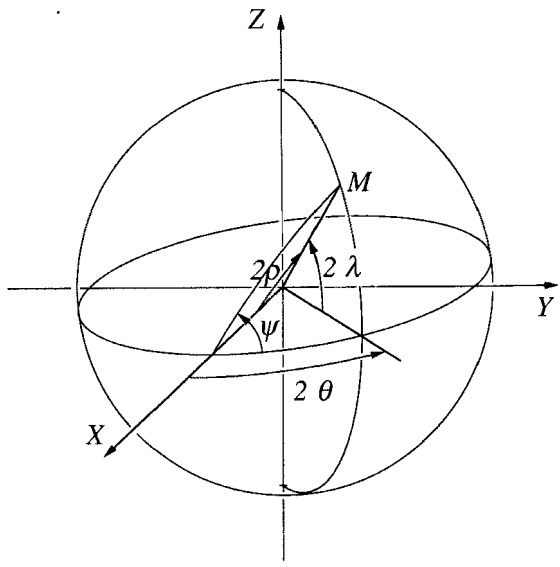

Figure 4. Representation on the Poincaré sphere of an elliptically polarized vibration (point M). Instead of angles $(2\theta, 2\lambda)$, one can choose angles $(\psi, 2\rho)$ to parameterize the light polarization on the sphere.

Downloaded At: 10:52 26 January 2011

Let 2ρ be the angle between $\mathbf{e}_X$ and $\mathbf{u}$ and ψ the angle of the dihedron formed by the equatorial plane and the plane containing $\mathbf{e}_X$ and point M (see figure 4). It is easy to show that the electric field can be written in the form:

$$\begin{cases} E_x = \cos\rho\cos\omega t, \\ E_y = \sin\rho\cos(\omega t - \psi). \end{cases} \tag{4}$$

3. Rotatory power of the TIC

In this section, we use some elementary properties of the Poincaré sphere to calculate the evolution of the electric field **E** through a TIC. Because this medium is one-dimensional and locally birefringent, it is convenient to replace it by a packing of thin, parallel, homogeneous slices perpendicular to the z axis. The conservation of the component of the electric field **E** parallel to the slices justifies this procedure.

3.1. *Evolution of the light polarization in a single homogeneous birefringent slice*

At the entrance of the slice, at $z=0$, the electric field is (4)

$$\begin{cases} E_x = \cos\rho\cos\omega t, \\ E_y = \sin\rho\cos(\omega t - \psi). \end{cases}$$

If the extinction directions of the slice are along x and y, a phase shift $\Delta\phi$ appears between E_x and E_y and, after crossing the slice, the electric field becomes

$$\begin{cases} E_x = \cos\rho\cos\omega t, \\ E_y = \sin\rho\cos(\omega t - \psi - \Delta\phi). \end{cases} \tag{5}$$

Consequently, the birefringent slice rotates the point M that represents the vibration on S^2 by an angle of $\Delta\phi$ around the x axis. The corresponding operator is the rotation matrix

$$B^0_{\Delta\phi} = \begin{pmatrix} 1 & 0 & 0 \\ 0 & \cos\Delta\phi & -\sin\Delta\phi \\ 0 & \sin\Delta\phi & \cos\Delta\phi \end{pmatrix}. \tag{6}$$

Suppose now that the extinction directions of the slice make an angle Θ in the x, y-plane with the x and y axes. The operator describing the motion of M on the Poincaré sphere is given by the matrix

$$B^\Theta_{\Delta\phi} = R_{2\Theta} B^0_{\Delta\phi} R_{-2\Theta}$$
$$= \begin{pmatrix} 1-\sin^2 2\Theta(1-\cos\Delta\phi) & \sin 2\Theta\cos 2\Theta(1-\cos\Delta\phi) & \sin 2\Theta\sin\Delta\phi \\ \sin 2\Theta\cos 2\Theta(1-\cos\Delta\phi) & 1-\cos^2 2\Theta(1-\cos\Delta\phi) & -\cos 2\Theta\sin\Delta\phi \\ -\sin 2\Theta\sin\Delta\phi & \cos 2\Theta\sin\Delta\phi & \cos\Delta\phi \end{pmatrix}, \tag{7}$$

where $R_{2\Theta}$ describes a rotation of angle 2Θ around the z axis. The matrix $B^\Theta_{\Delta\phi}$ corresponds to a rotation of angle $\Delta\phi$ around the unit vector $\mathbf{v} = (\cos 2\Theta, \sin 2\Theta, 0)$.

In the limit of an infinitely thin slice of thickness dz, the vector $\mathbf{u} = \mathbf{OM}$ becomes $\mathbf{u} + \mathbf{du}$ after the light has crossed the slice with

$$\mathbf{du} = \mathbf{v} \wedge \mathbf{u}\, d\phi, \tag{8}$$

where $d\phi$ is the phase shift between E_x and E_y.

3.2. *One-dimensional medium*

3.2.1. *General points*

A one-dimensional medium can be described by the stacking-up of such birefringent homogeneous slices. Since the product of two rotations is a rotation, the operator describing the change of polarization of a light beam propagating across a one-dimensional medium is a rotation [9]. Contrary to the previous case of a homogeneous birefringent medium, the axis of the rotation is no longer necessarily in the equatorial plane of the Poincaré sphere. Nevertheless, it is always possible to factor this rotation into two successive rotations whose axes are respectively in the equatorial plane (homogeneous birefringent medium) and along the pole axis (medium with a pure rotatory power). A one-dimensional medium can thus always be described as the superposition of a homogeneous birefringent medium and a medium with a pure rotatory power. This second fictitious medium rotates all the vibrations by an angle $\Delta\theta$, independently of their initial polarization. The angle $\Delta\theta$ is thus characteristic of the one-dimensional medium. It can be obtained by a simple geometrical construction on the Poincaré sphere (see figure 5) by considering the image of the equator under the rotation operator associated with the real medium. This image is a great circle which intersects the equator at two opposite points P_1 and P_2. These points are the images of two particular points M_1 and M_2 corresponding to vibrations that are linearly polarized in two perpendicular directions of the real space. It is possible to show that $\Delta\theta$ is equal to the half-angle between $\mathbf{OP}_1$ and $\mathbf{OM}_1$ (or between $\mathbf{OP}_2$ and $\mathbf{OM}_2$). We choose $\Delta\theta$ positive if the medium is *dextrorotatory* (Pasteur's convention). We shall determine this quantity in the following.

Downloaded At: 10:52 26 January 2011

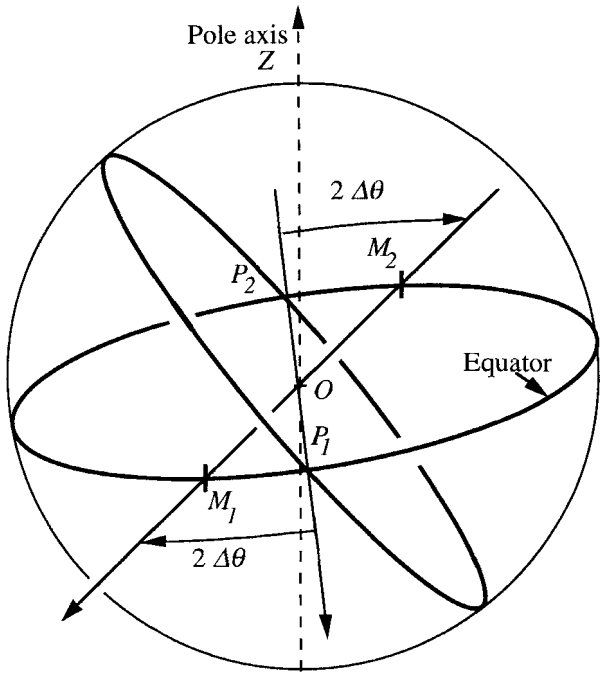

Figure 5. Poincaré sphere representation of the existence of two orthogonal positions of the polarizer for which the light emerging from the one-dimensional medium is still linearly polarized and can be extinguished with an analyser. The angle between the polarizer and the analyser for which we get complete extinction is $\pi/2+\Delta\theta$.

Downloaded At: 10:52 26 January 2011

In conclusion, there exist two particular orientations of the polarizer (corresponding to points M_1 and M_2 on the sphere) for which the light emerging from the medium is still linearly polarized (points P_1 and P_2 on the sphere). Under these conditions, it is possible, by use of the analyser of the microscope, to obtain optical extinction of the sample.

3.2.2. *Free cholesteric*

The first example of a one-dimensional medium is the non-constrained cholesteric liquid crystal (or twisted nematic)

$$\mathbf{n} \begin{vmatrix} \cos qz \\ \sin qz \\ 0 \end{vmatrix} \tag{9}$$

with $q=2\pi/p$. According to equation (9), the expression of the vector $\boldsymbol{v}$ defined in § 2 reads

$$\boldsymbol{v} \begin{vmatrix} \cos 2qz \\ \sin 2qz \\ 0 \end{vmatrix} \tag{10}$$

while the phase difference after crossing a slice of thickness dz is

$$d\phi = -\Delta n \frac{2\pi}{\lambda_0} dz. \tag{11}$$

Our purpose in this sub-section is to show that there exist particular thicknesses for which the sample has a true rotatory power. In order to show this property, let us first describe two particular and independent solutions of equation 8.

The first solution was found by Mauguin [1]. It describes the evolution of the polarization in the Poincaré sphere, when the incident beam is *linearly polarized along an extinction direction* at $z=0$ (for instance parallel to the molecules). This initial polarization is represented by the point A on the sphere such that $\mathbf{OA}=\mathbf{e_x}$. Let B be the point corresponding to the extinction direction parallel to the molecules at $z=d$. The point M giving the evolution of the light polarization across the sample is fixed on a cone that rolls without gliding on the equatorial plane from **OA** to **OB**. This point is identical with A at the input of the medium ($z=0$). The half-aperture angle of this cone Ω depends on the birefringence Δn, on the cholesteric pitch p, and on the wavelength λ_0

$$\tan\Omega=\frac{2}{\Delta n}\frac{\lambda_0}{p}. \tag{12}$$

A second particular solution to this problem is (equations (8), (10) and (11)):

$$\mathbf{u}=\cos\Omega\mathbf{v}+\sin\Omega\mathbf{e_z} \tag{13}$$

In this case, point M describes a circle parallel to the equator on the sphere. The polarization at $z=0$ is no longer rectilinear and is represented by the point A' on the sphere such that **OA'** is in the plane containing **OA** and the pole axis.

We show now that if the sample thickness is a multiple of $(p/2)\sin\Omega$, any initial linearly polarized vibration remains linearly polarized after traversing the sample, which means that the sample has a pure rotatory power.

Let us first consider the Mauguin solution. If $d=(p/2)\sin\Omega$, the Mauguin cone spins exactly once upon itself. Since the initial vibration is polarized along an extinction direction, the emerging vibration at $z=d=(p/2)\sin\Omega$ is also linearly polarized, which means that its representative point on the Poincaré sphere has rotated by an angle $2\pi\sin\Omega$ around the pole axis. Let us now consider the second particular solution given by equation 13 (independent of the previous one). In this case, the point M representing the polarization on the Poincaré sphere rotates between $z=0$ and $z=d=(p/2)\sin\Omega$ of the angle $2\pi\sin\Omega$ around the pole axis, as in the previous case. Consequently, the effect of a sample of thickness $m(p/2)\sin\Omega$, $m\in\mathbb{N}$ on any light polarization is a rotation by an angle $2\pi m\sin\Omega\ (\mathrm{mod}\ 2\pi)$ around the pole axis. That means that an incident linearly polarized beam remains linearly polarized after crossing the sample which therefore has a true rotatory power.

We shall speak about an *extinction point* each time this property is satisfied, because it is then possible to obtain optical extinction of the sample with the analyser for any position of the polarizer. These *extinction conditions* are optimal for measuring the angle of rotation of the polarization.

3.2.3. *Generalization to the TIC*

In this sub-section, we explain the method by which the TIC is calculated and we show how to determine the angle of rotation of light polarization. In particular, we shall show that the *extinction points* are not specific to free cholesterics, but can also be observed in a TIC.

Downloaded At: 10:52 26 January 2011

We consider a cholesteric sandwiched between two plates, at $z=0$ and $z=d$, imposing homeotropic anchoring. In the TIC, the director field reads

$$\mathbf{n}\left|\begin{array}{l} n_x=\sin\alpha(z)\sin\beta(z) \\ n_y=\sin\alpha(z)\cos\beta(z) \\ n_z=\cos\alpha(z) \end{array}\right. \tag{14}$$

The exact form of α and β can be found by minimizing the Frank energy

$$F=\tfrac{1}{2}K_1(\nabla\cdot\mathbf{n})^2+\tfrac{1}{2}K_2(q+\mathbf{n}\cdot(\nabla\times\mathbf{n}))^2+\tfrac{1}{2}K_3(\mathbf{n}\times(\nabla\times\mathbf{n}))^2-\frac{\varepsilon_a}{2}(\mathbf{E}\cdot\mathbf{n})^2 \tag{15}$$

where we assume that the electric field is constant and equal to V/d inside the sample. The α and β were first calculated by Fischer analytically [10], and are solutions of the system of equations

$$\begin{aligned} &\ddot{\alpha}(K_{12}\sin^2\alpha+K_{32}\cos^2\alpha)+(K_{12}-K_{32})\dot{\alpha}^2\sin\alpha\cos\alpha \\ &=4AV^2\sin\alpha\cos\alpha+2(2C+\sin^2\alpha\dot{\beta})\sin\alpha\cos\alpha\dot{\beta} \\ &+\dot{\beta}^2K_{32}\sin\alpha\cos\alpha(\cos^2\alpha-\sin^2\alpha) \end{aligned} \tag{16}$$

and

$$\dot{\beta}=-\frac{2C}{\sin^2\alpha+K_{32}\cos^2\alpha},$$

with

$$\dot{}=\frac{d}{\pi}\frac{d}{dz},\quad C=\frac{d}{p},\quad K_{32}=\frac{K_3}{K_2},\quad K_{12}=\frac{K_1}{K_2},\quad A=\frac{\varepsilon_a}{4\pi K_2}.$$

The boundary conditions of strong homeotropic anchoring impose $\alpha(0)=\alpha(d)=0$. It is obvious from equation (16) that the structure of the TIC tends to that of the free cholesteric previously described when $V\to+\infty$. From these results, it is possible to show that the TIC–nematic transition is second order when

$$C<\frac{K_{32}}{2}\left[\frac{K_{12}}{3(K_{32}-1)}\right]^{1/2} \quad [11].$$

To calculate the evolution of the light polarization, we can use the general equation (8). In the case of the TIC we obtain

$$\mathbf{v}\left|\begin{array}{c} -\cos 2\beta \\ \sin 2\beta \\ 0 \end{array}\right. \tag{17}$$

and

$$d\phi=\frac{2\pi}{\lambda_0}(n_0-n'(\alpha))dz, \tag{18}$$

with

$$n'(\alpha)=\frac{n_e n_o}{[n_e^2+(n_o^2-n_e^2)\sin^2\alpha]^{1/2}},$$

Downloaded At: 10:52 26 January 2011

where n_e (and n_o) is the extraordinary (and ordinary) refractive index. Let us parameterize $\mathbf{u}$ by the angles θ and λ such that

$$\mathbf{u} \begin{vmatrix} \cos 2\lambda \cos 2\theta \\ \cos 2\lambda \sin 2\theta \\ \sin 2\lambda \end{vmatrix} \tag{19}$$

Using expressions (8), (17) and (18), we obtain the system of equations

$$\begin{cases} \dfrac{d(2\theta)}{dz} = \dfrac{2\pi}{\lambda_0}(n_0 - n'(\alpha)) \tan 2\lambda \cos(2\theta + 2\beta) \\ \dfrac{d(2\lambda)}{dz} = -\dfrac{2\pi}{\lambda_0}(n_o - n'(\alpha)) \sin(2\theta + 2\beta). \end{cases} \tag{20}$$

with the initial conditions $\theta\,(z=0)=\theta_0$, $\lambda\,(z=0)=0$, which correspond to an incident linearly polarized vibration, the system (20) has a single solution $(\theta(z,\theta_0), \lambda(z,\theta_0))$. Set $\mathbf{u}_0 = \cos 2\theta_0 \mathbf{e}_X + \sin 2\theta_0 \mathbf{e}_Y$. To know the output polarization at $z=d$ for any value of θ_0, it is sufficient to solve equation (20) for two particular values of θ_0, for instance $\theta_0=0$ and $\theta_0=\pi/4$. This is due to the fact that the rotation R describing the action of the TIC on the light polarization is a linear operator so that $R(\mathbf{u}_0) = \cos 2\theta_0 R(\mathbf{e}_X) + \sin 2\theta_0 R(\mathbf{e}_Y)$. This relation can be rewritten in the form:

$$\begin{aligned} \sin 2\lambda(d,\theta_0) &= \sin 2\lambda(d,0)\cos 2\theta_0 + \sin 2\lambda\left(d,\frac{\pi}{4}\right)\sin 2\theta_0 \\ \cos 2\lambda(d,\theta_0)\cos 2\theta(d,\theta_0) &= \cos 2\lambda(d,0)\cos 2\theta(d,0)\cos 2\theta_0 \\ &\quad + \cos 2\lambda\left(d,\frac{\pi}{4}\right)\cos 2\theta\left(d,\frac{\pi}{4}\right)\sin 2\theta_0 \\ \cos 2\lambda(d,\theta_0)\sin 2\theta(d,\theta_0) &= \cos 2\lambda(d,0)\sin 2\theta(d,0)\cos 2\theta_0 \\ &\quad + \cos 2\lambda\left(d,\frac{\pi}{4}\right)\sin 2\theta\left(d,\frac{\pi}{4}\right)\sin 2\theta_0 \end{aligned} \tag{21}$$

The values $\bar{\theta}_0$ and $\bar{\theta}_0 + \pi/2$ of the angle θ_0 corresponding to the points M_1 and M_2 introduced in the beginning of this subsection (see also figure 4) can be obtained by setting $\lambda(d,0)=0$ in equation (21). This gives

$$\tan 2\bar{\theta}_0 = -\frac{\sin 2\lambda(d,0)}{\sin 2\lambda(d,\pi/4)}. \tag{22}$$

In these two particular cases of initial polarization (given by M_1 and M_2 on the sphere), the light is still linearly polarized after it has crossed the TIC. The angle of rotation of the polarization, measurable experimentally when the incident beam is polarized along M_1 or M_2 on the sphere, and defined to be

$$\Delta\theta = \bar{\theta}_0 - \theta(d,\bar{\theta}_0) \tag{23}$$

can then be calculated from equation (21) and (22).

We can also determine the *extinction points* by solving the equations $\lambda(d,0) = \lambda(d,\pi/2) = 0$ as a function of the experimental parameters d and V. Under these special

Downloaded At: 10:52 26 January 2011

conditions, the light is always linearly polarized at the output of the TIC, independently of the initial polarization. Furthermore, the angle of rotation of polarization is independent of the initial polarization, which means that the medium has a true rotatory power.

3.3. *Numerical results*

We have chosen as numerical parameters

$$K_{32} = 1{\cdot}97,$$
$$A = -0{\cdot}138\ \mathrm{V}^{-2},$$
$$n_e = 1{\cdot}5183,$$
$$n_e - n_o = 0{\cdot}0437.$$

These values, given E. Merck correspond to the left-handed mixture described in the introduction and used in [6]. The quiescent cholesteric pitch of this mixture is equal to 15·7 μm and was measured by the Cano-wedge method. We evaluated K_{12} in [6] by fitting the experimental phase diagram with the theoretical one. We found $K_{12} \approx 1{\cdot}62$. The wavelength of the green filter chosen is $\lambda_0 = 546$ nm.

These data allow us to calculate the angle of rotation $\Delta\theta$ of the polarization in a TIC as a function of C and V. The calculations were done for small sample thickness ($C \leqslant 0{\cdot}6$), when the TIC–homeotropic nematic phase transition is second order (see the phase diagram of figure 1). The TIC is always found numerically to be laevorotatory (according to the usual optics conventions), which means that the electric field rotates in the sense opposite to that of the cholesteric helix. In figure 6, we plotted the angle $|\Delta\theta|$ characterizing the optical activity of the TIC as a function of C and V. For each value of

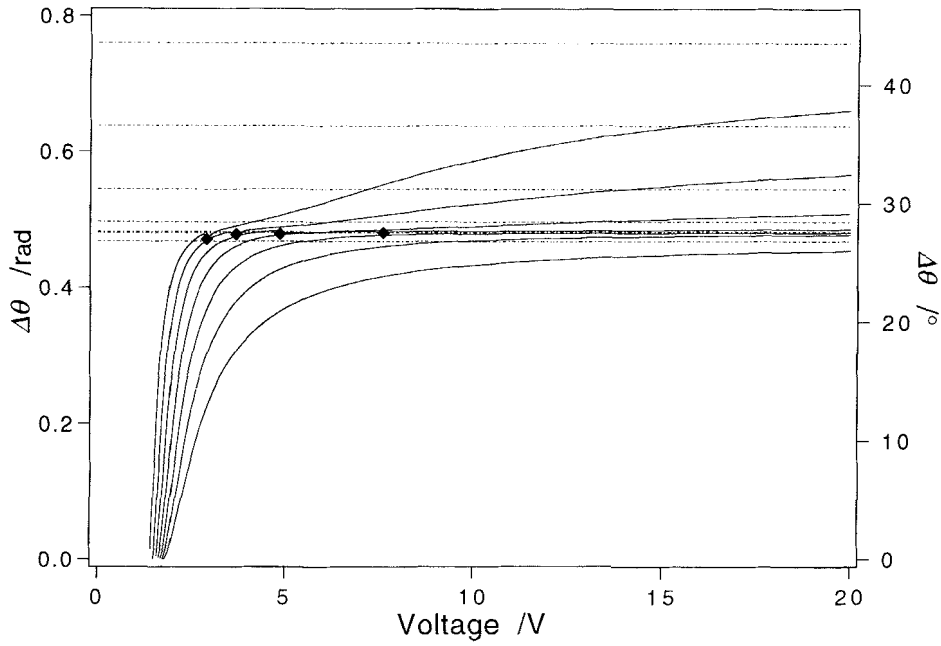

Figure 6. Rotation angle of the polarization $\Delta\theta$ versus the applied voltage for different sample thicknesses. From the top to the bottom, $C = 0{\cdot}65$, 0·6, 0·55, 0·5, 0·45, 0·4 and 0·35. The extinction points (represented by solid diamonds) correspond from left to right to $C = 0{\cdot}65$, 0·6, 0·55, 0·5. (——), numerical calculation; (· · ·), numerical calculation at infinite voltage.

Downloaded At: 10:52 26 January 2011

C, $|\Delta\theta|$ tends asymptotically towards a finite value which corresponds to the limiting case of the free cholesteric phase. We have also plotted on the curves of figure 6 the positions of the *extinction points* found numerically at $C \geqslant 0{\cdot}5$.

In order to test the accuracy of our numerics, we have calculated the value of $\Delta\theta$ at the extinction point for a free cholesteric. The values we have found, $C = 0{\cdot}423$ and $|\Delta\theta| = 0{\cdot}482$ rad, are in excellent agreement with those given by an analytical calculation

$$C = \tfrac{1}{2}\sin\Omega, \quad |\Delta\theta| = 2\pi(1-\sin\Omega) \quad \text{and} \quad \tan\Omega = \frac{2}{\Delta n}\frac{\lambda_0}{p}.$$

It is important to note that this value of $\Delta\theta$ is different from that given by the classic formula of de Vries. This difference is due to the fact that the classic formula is only applicable when $(\Delta np/\lambda_0) \ll 1$, whereas, in our experiment, this quantity equals 1·26.

3.4. *Experimental results*

Our experimental set up has been described in [6] and [12]. The mixture, the temperature chosen (30°C), and the frequency of the applied square-wave AC voltage (5 kHz) were the same as in [6]. We used a green interference filter (546 nm) to perform all the measurements.

We measured the angle of rotation of the polarization $\Delta\theta$, by looking for one of the two particular positions of the polarizer and of the analyser for which the TIC is completely dark. In fact, this extinction is rarely observed across a large surface area, because the molecular tilt direction can vary spatially in the sample plane. This effect

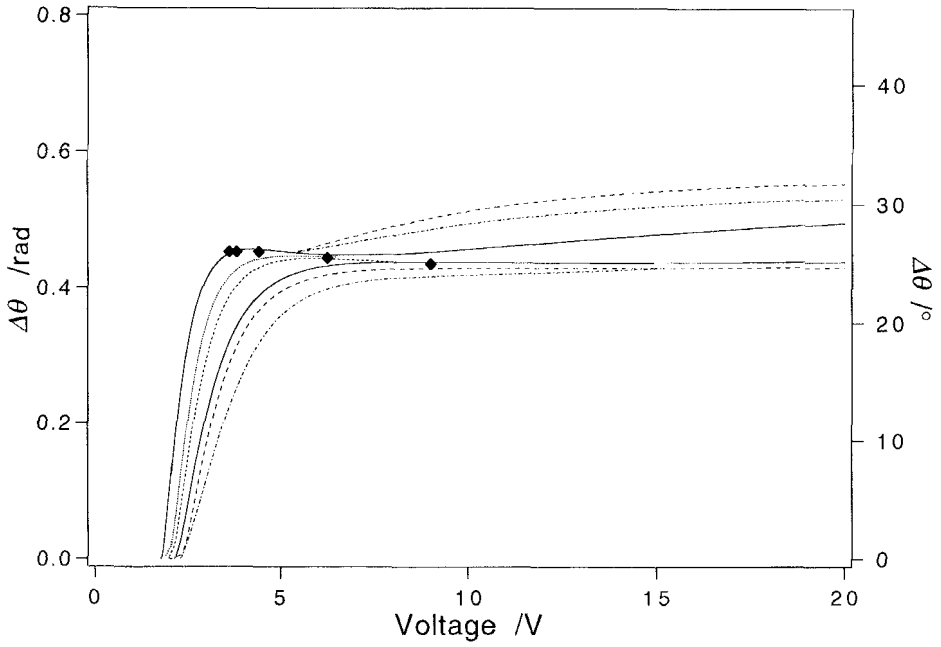

Figure 7. Rotation angle of the polarization $\Delta\theta$ versus the applied voltage for different sample thicknesses: experimental results. From top to bottom: ((– – –), C = 0·625; (– · – · –), C = 0·600; (——), C = 0·560; (· · · · · · ·), C = 0·512; (- - - - -); C = 0·463; (——), C = 0·413; (– – – –), C = 0·365; (· – · – · –), C = 0·320. The extinction points (represented by solid diamonds) correspond from left to right to $C = 0{\cdot}625$, 0·6, 0·56, 0·512 and 0·663.

Downloaded At: 10:52 26 January 2011

and the difficulty of finding the positions of the polarizers for which the local extinction is most complete lead to an uncertainty in the $\Delta\theta$ measurement of about one degree. On the other hand, it is sometimes possible to obtain perfect extinction over the whole sample area, even when the TIC is inhomogeneous. These peculiar experimental conditions correspond to the *extinction points* predicted theoretically (see § 3.2).

In figure 7, we plotted $\Delta\theta$ as a function of the voltage V for different thicknesses. We also indicated the positions of the extinction points. We find that the TIC is laevorotatory and that the angle of rotation increases with the thickness and the voltage. All these results are in good agreement with the numerical results of figure 6, in particular the positions of the extinction points. For instance, at $C=0{\cdot}6$ we measured $V_{ext}=3{\cdot}60$ V while the calculation gives $V_{ext}=3{\cdot}70$ V. Furthermore, we found experimentally that there is no extinction point when $C\leqslant 0{\cdot}41$, in very good agreement with the theory. Note that there is no adjustable parameter in our calculations. Consequently, our approximation that the electric field remains constant and perpendicular to the glass plates inside the sample seems rather good.

We now extend our model to the cholesteric fingers in order to calculate their optical contrast between crossed polarizers. Our main motivation was to confirm the topological model used in [6].

Downloaded At: 10:52 26 January 2011

4. Optical contrast of the cholesteric fingers

4.1. *Experimental results*

Figure 8 shows an array of parallel fingers at $V=0$ photographed between crossed polarizers. In order to obtain a normal illumination, we removed the condenser of the microscope. In this case, the optical contrast of the fingers does not change as long as we focus inside the sample. This is due to the very small birefringence of the mixture chosen ($\Delta n=0{\cdot}0437$) and to the fact that the deviation angle of the light across the sample is always negligible (less than 2° in our samples [11]). In figure 9(*a*), we reported measurements of the intensity profile along the normal to the finger axis, when the polarizer and the analyser are perpendicular. These profiles are symmetrical when the finger axis makes an angle of 0°, 45° or 90° with the polarizer and asymmetrical otherwise. In this figure, we have normalized the light intensity: the value 0 (resp. 1) corresponds to the intensity of the homeotropic nematic phase observed between crossed polarizers (resp. between parallel polarizers).

We also observed that it was always possible to extinguish locally the fingers by decrossing the polarizer and the analyser. This allowed us to measure the local rotation angle of the polarization $\Delta\theta$ along the normal to the finger axis (figure 10(*a*)). This property of the fingers shows that they behave at each point as a one-dimensional medium and comes from the fact that the light is not strongly deviated inside the sample.

4.2. *Director field inside a finger*

In [6], we proposed that the director field inside the fingers should be decreased by

$$\left|\begin{aligned} n_x &= \cos\beta\sin\gamma\sin ky-\cos\alpha\sin\beta\sin\gamma\cos ky+\sin\alpha\sin\beta\cos\gamma\\ n_y &= -\sin\beta\sin\gamma\sin ky-\cos\alpha\cos\beta\sin\gamma\cos ky+\sin\alpha\cos\beta\cos\gamma\\ n_z &= \sin\alpha\sin\gamma\cos ky+\cos\alpha\cos\gamma \end{aligned}\right. \tag{24}$$

where k is the wavevector ($k=2\pi/\Lambda$ and Λ is the finger width) and α, β, γ are three angles such that

$$\left|\begin{array}{l}\alpha(z=0)=\alpha(z=d)=0\\ \gamma(z=0)=\gamma(z=d)=0\end{array}\right. \tag{25}$$

These conditions ensure homeotropic anchoring on the glass plates. The x axis is assumed to be parallel to the finger axis while the y axis is perpendicular to it. Formula (24) describes the nematic when $\alpha=\gamma=0$, the TIC when $\alpha\neq 0$ and $\gamma=0$, and the fingers (here considered as a periodic modulation of the TIC) when α and γ are both different from 0. The case $\alpha=\gamma\neq 0$ corresponds to fingers separated by the homeotropic nematic

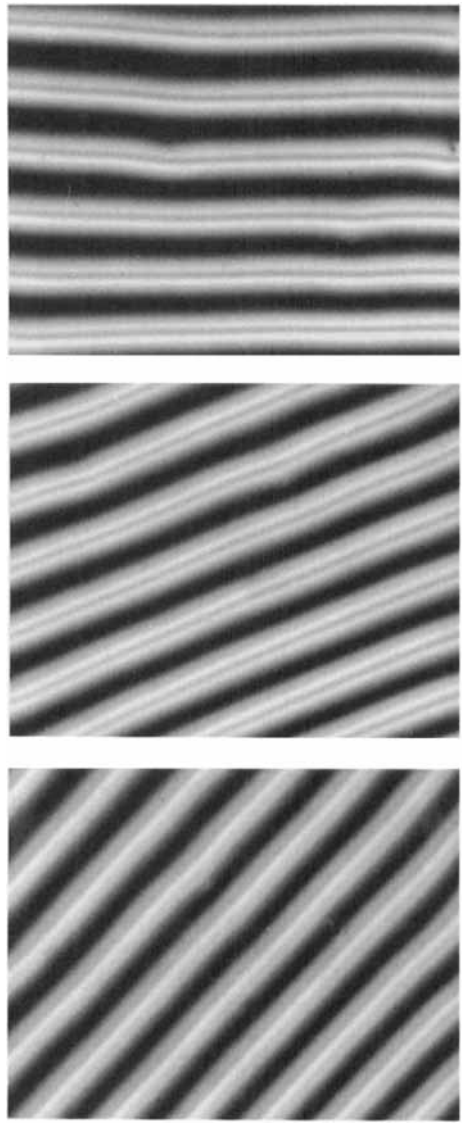

(*a*)

(*b*)

(*c*)

Downloaded At: 10:52 26 January 2011

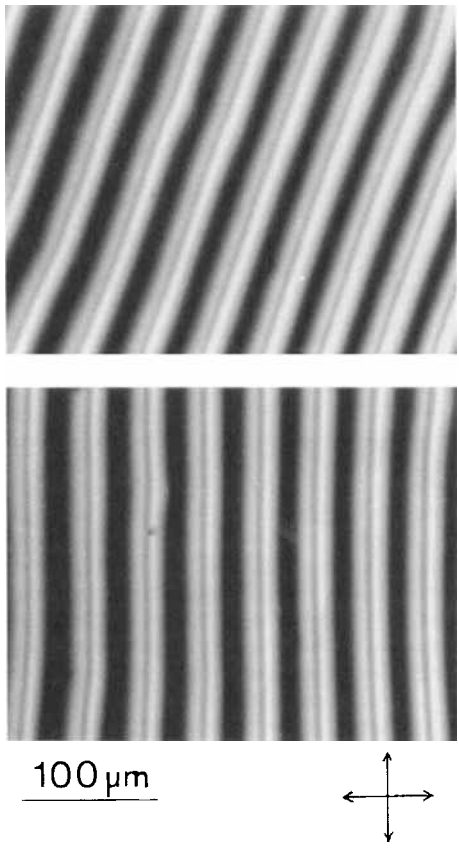

Figure 8. Parallel fingers photographed between crossed polarizers. Their contrast changes when the sample is turned around the optical axis of the microscope. ($C=1{\cdot}15$, $V=0$ V). The angles between the finger axis and the polarizer are (*a*) 0°, (*b*) 20°, (*c*) 45°, (*d*) 70° and (*e*) 90°.

Downloaded At: 10:52 26 January 2011

phase. By minimizing the free energy (15) with respect to α, β and γ, it was possible to show that the solution can be written in the form [6]

$$\left.\begin{aligned}\alpha &= \alpha_0 \sin Z \\ \beta &= \frac{2C}{K_{32}}\left(\frac{\pi}{2} - Z\right) \\ \gamma &= \gamma_0 \sin Z\end{aligned}\right\} \tag{26}$$

with $Z = \pi z/d$. These formulae are only exact in the vicinity of the critical line when the transition is second order, i.e. between points A and B in phase diagram of figure 2. Nevertheless, we assumed in [6] that they could still be used far from this line. In this case, it was possible to calculate the energy per unit surface area of the sample and to minimize it with respect to k and to (α_0, γ_0), which plays the role of a two-dimensional order parameter. In this way, it was possible to establish a theoretical phase diagram in satisfactory agreement with the experimental one.

In order to test the validity of this theoretical approach, we have calculated the optical contrast of the fingers when they are observed between crossed polarizers as

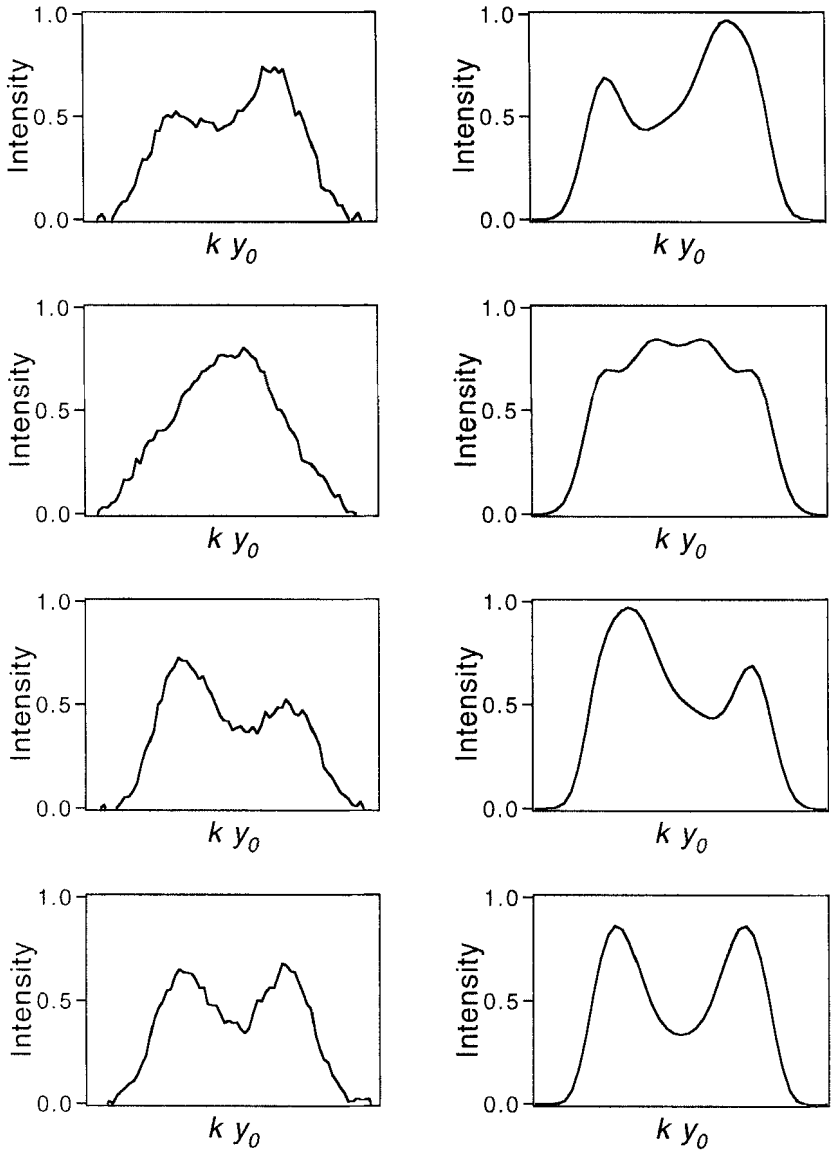

Figure 9. (*a*) Experimental ($C=1{\cdot}15$, $V=0$ V) and (*b*) theoretical ($C=1{\cdot}13$, $V=0$ V) intensity profiles $I_\perp(y_0)$. From top to bottom, the angle between the polarizer and the finger axis successively equals 70°, 45°, 20° and 0°.

Downloaded At: 10:52 26 January 2011

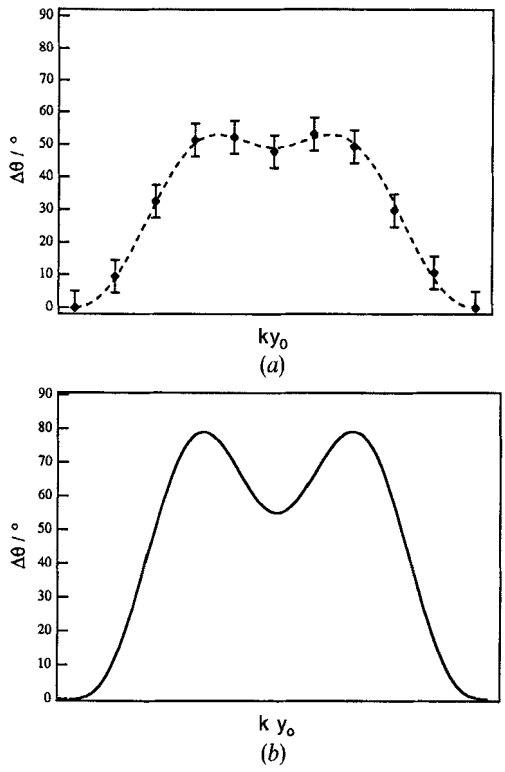

Figure 10. (*a*) Experimental ($C = 1{\cdot}15$, $V = 0$ V) and (*b*) theoretical ($C = 1{\cdot}13$, $V = 0$ V) rotation angle of the polarization $\Delta\theta$ versus y_0.

Downloaded At: 10:52 26 January 2011

well as their local rotatory power. We have used the director field (24)–(26) and the values of (α_0, γ_0) which minimize the free energy. In the following sub-section, we explain the details of these calculations.

4.3. *Calculations of the optical contrast between crossed polarizers and of the rotation angle of the polarization* $\Delta\theta$

The previous model used to calculate the optical properties of the TIC is, a priori, not immediately applicable to the fingers, because these solutions are not one-dimensional. Indeed, the horizontal index variations induce deviations of the light rays. The thicker and more birefringent the sample, the more important the deviations are. Taking this effect into account is very difficult, and we did not attempt to do that. On the other hand, we have observed experimentally that the deviations are very small. This is due to the fact that the quantity $\Delta nd/\Lambda$ (where Λ is the finger width), which measures the maximum deviation angle, is always much smaller than 1.

Consequently, one can consider a finger to be a pile of thin slices perpendicular to the glass plates and parallel to the finger axis, in which the rays propagate without deviation as they would do in the corresponding one-dimensional medium.

More precisely, let us consider a slice of coordinate y_0. Along the line (parallel to the finger axis), the behaviour is that of a one-dimensional medium in which the director field is

$$\mathbf{n}(z) = \mathbf{n}_{\text{finger}}(y_0, z) \tag{27}$$

where $\mathbf{n}_{\text{finger}}$ is given by equation (24)–(26). In order to calculate the polarization of the light after it has crossed the slice, we solve equation (20) numerically by using a Runge–Kutta method with the initial conditions: $\theta(z=0)=\theta_0$, $\lambda(z=0)=0$. These conditions correspond to an incident vibration linearly polarized at an angle θ_0 with the finger axis. This polarization is represented on the sphere by a vector $\mathbf{u}_0$. Let us call $\mathbf{u}_d(y_0)$ the unit vector representing the polarization of the light on the Poincaré sphere at the output of the medium: the transmitted intensity $I_\perp$ between crossed polarizers is

$$I_\perp(y_0)=I_0(1-\mathbf{u}\cdot\mathbf{u}_d(y_0)), \tag{28}$$

where I_0 is a constant. If the polarizers are parallel, one calculates in the same way

$$I_\parallel(y_0)=I_0(1+\mathbf{u}_0\mathbf{u}_d(y_0)). \tag{29}$$

Consequently, one must take $I_0=1/2$ in keeping with the normalization of the intensity chosen in the experimental part (see § 4.1).

In figure 9(*b*), we have plotted the calculated intensity profiles between crossed polarizers for different values of the angle θ_0 between the polarizer and the finger axis. These profiles have been calculated by assuming $\alpha_0=\gamma_0$ (the sides of the fingers are homeotropic) and by looking for the values of C and α_0 for which the intensity in the middle of the finger is the same as that measured experimentally when the finger makes angles of 0 and $\pi/4$ with the polarizer. This procedure gives $C=1{\cdot}13$ and $\alpha_0=1{\cdot}12$ rad and leads to profiles that are in satisfactory agreement with the experimental ones (see figure 9). This value of C is in good agreement with the experimental one: $C=1{\cdot}15$. By contrast, the value of α_0 is 30 per cent larger than that we have obtained after minimization of the free energy: α_0 (theory) $=0{\cdot}85$ rad.

The same model can be used for calculating the rotation angle of the polarization $\Delta\theta$ as a function of coordinate y_0. The corresponding theoretical curve is plotted in figure 10(*b*) by taking the same values $C=1{\cdot}13$ and $\alpha_0=1{\cdot}12$ rad as previously. This curve has the same shape as that measured experimentally, but predicts maximal values of $\Delta\theta$ that are too large by about 30 per cent. This disagreement is not however surprising in view of the numerous approximations we have made.

5. Conclusion

We have studied the optical properties of the two classical textures observed for thin samples of a cholesteric liquid crystal of negative dielectric anisotropy submitted to homeotropic anchoring and to an electric field.

The first solution (TIC) is translationally invariant in the sample plane and rotates the light polarization. Using the Poincaré sphere, we have calculated the rotatory power of the TIC. In general, this quantity is only defined for two orthogonal directions of the polarizer. Nevertheless, if the sample is sufficiently thick, there exist particular values of the applied voltage for which the sample has a true rotatory power. In these conditions, called *extinction points*, it is possible to obtain complete extinction of the sample with the analyser, whatever the position of the polarizer. All these theoretical predictions have been verified experimentally. The agreement between theory and experiment is excellent in spite of the assumption that the electric field is constant throughout the sample. We also emphasize that there is no adjustable parameter in our model.

We have then tried to extend our optical model to the case of the fingers. Calculations are much more complicated in this case and much less precise, because we do not know the exact director field inside a finger. Thus, calculations were done by

Downloaded At: 10:52 26 January 2011

using the topological model of [6] which assumes that the fingers have no singularity inside and can be constructed from a continuous modulation of the TIC. We also assumed that the rays do not deviate within the finger, which limited our calculations to the case where $\Delta nd/\Lambda \ll 1$, i.e. in practice $\Delta n \ll 1$. This condition was fulfilled in our experiment. In order to obtain direct comparison with experiment, we calculated the optical contrast of the fingers between crossed polarizers as well as their local rotatory power. The intensity profiles that we found for different positions of the polarizers with respect to the finger axis and the curve of the rotatory power are in good qualitative agreement with experiment.

This work was supported by DRET Contract No. 92/1313/DS/SR.

References

[1] MAUGUIN, CH., 1911, *Bull. Soc. fr. Minér. Cristallogr.*, **34,** 71.
[2] OSEEN, C. W., 1933, *Trans. Faraday Soc.*, **29,** 833.
[3] DE VRIES, Hl., 1951, *Acta crystallogr.*, **4,** 219.
[4] DE GENNES, P. G., 1974, *The Physics of Liquid Crystals* (Oxford University Press), pp. 219–236.
[5] GOOD, R. H. JR., 1992, *J. Phys. Cond. Matter*, **4,** 1623.
[6] RIBIÈRE, P., PIRKL, S., and OSWALD, P., 1991, *Phys. Rev.* A, **44,** 8192.
[7] LEQUEUX, F., 1988, *J. Phys., France*, **49,** 967.
[8] POINCARÉ, H., 1892, *Théorie mathématique de la lumière* (Gauthier Villars).
[9] MAUGUIN, CH., 1911, *Bull. Soc. fr. Minér. Cristallogr.*, **34,** 6.
[10] FISCHER, F., 1976, *Z. Naturf.* (*a*); **31,** 41.
[11] RIBIÈRE, P., 1992, Thesis, Université Claude Bernard-Lyon I, Order No 289.92, p. 47.
[12] RIBIÈRE, P., and OSWALD, P., 1990, *J. Phys., France*, **51,** 1703.

Downloaded At: 10:52 26 January 2011